

# STRUCTURAL RESPONSE TO IMPACT LOADS WITH SOIL-STRUCTURE INTERACTION

A.F. Abdel Rahman, M.R. Shehata,  
L. EL-Hifnawy and H.N. El-Shrif

Civil Engineering Department, Faculty of Engineering,  
Alexandria University, Alexandria, Egypt.

## ABSTRACT

A theoretical study, of the dynamic behaviour of structures subjected to impact load, such as blast impact load and vehicle impact load is presented. Five, ten and fifteen storey shear buildings resting on flexible foundations are investigated. Using the substructure approach, the equations of motion of the soil-structure interaction system are determined. These equations are solved, both in the time domain and in the frequency domain using the non-classical modal analysis and the complex response analysis respectively. The analysis indicates that the first mode of vibration controls the response for the case of blast load impacting the top floor of the structures. For the case of vehicle load impacting the first floor of the same buildings, the response is controlled by higher modes of vibrations. The higher the building is, the greater is its maximum dynamic response, for the case of load impacting the top of the building. But for the case of the load impacting the bottom of the building, the higher the structure, the lower is its dynamic response.

*Keywords: Soil, Structure interaction, impact load, shear Building, Vehicle impact, blast load, dynamic response.*

## 1. INTRODUCTION

Many types of structures are subjected to transient dynamic forces that are quite short in duration and can be characterized as pulses or shocks. Typical examples of such loading involve impact related accidents with these structures such as vehicle impact, tornado-tossed objects impacts, aircraft collision, and blast loading. The forces generated in such structures are often very powerful and can result in many undesirable effects such as cracking, or, local crushing of the structure.

The development of the nuclear reactor has led to a growing concern over possible safety hazards related to nuclear structures, prompting research in the area of nuclear power plants subjected to aircraft collisions (1 to 3). More recently, impacts by large projectiles such as passenger vehicles (4 to 7) have been studied. In this area, the dynamic response of a steel Barrier panel struck by a wind-tossed vehicle (6) is examined. As an extension of this research, a

similar impact was simulated with a reinforced concrete structure similar to that used in wall and roof design of reactor auxiliary buildings. The dynamic response was investigated by using the modal and direct integration procedures (7).

Concern, also, exists over the potential danger associated with the problem of blast explosions (8 to 10). Information about the developments in this field is made available mostly through publications of the Army Corps of Engineers, Department of Defense, U.S. Air Force. Much of the work is done by the Massachusetts Institute of Technology, the University of Illinois and other leading institutions and engineering firms. It should be pointed that structures cannot be protected from a direct hit by a bomb, but it can, however, be designed to resist the blast pressures when it is located at some distance from the point of explosion.

In this research, structural response to impact load,

such as, vehicle impacts and blast load impacts of shear buildings having different heights are investigated. Two methods of analysis are used in which damping is accounted for in a rigorous way. The first method, is the complex eigenvalue approach, which is a mathematically accurate time-domain solution, (11 to 15). The second approach is the complex response analysis, where the solution can be conducted in the frequency domain using the very efficient fast Fourier transform, (16 to 18). Examples as well as comparisons between the two approaches are given.

2. IMPACT LOADS

**Vehicle impact load:** Figure (1-a) shows the force-time relationship associated with the actual impact of a structure with standard-size 4000-lb (1800-kg) passenger vehicle, at 130 mph (210 km/hr) speed. According to (7), the worst impact condition was assumed with the vehicle velocity vector normal to the impacted structure. The total load duration is 120 milli-seconds, with a maximum value of 150 psi (1000 kpa), and a contact area of 36x72 in (0.9x1.82m).

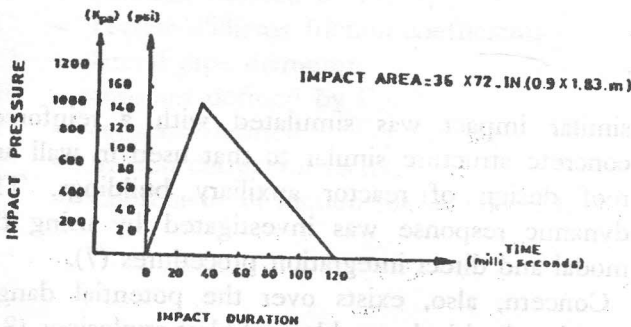


Figure 1-a. Vehicle impact load.

**Blast Impact Load:** In general, a blast explosion is the result of a very rapid release of large amounts of energy due to chemical reactions that involve a rearrangement among the atoms. Figure (1-b) shows an averaged loading due to a blast wave with 20 kpa peak over-pressure and 200 milli-seconds duration (10). The load begins with an infinite steep rise from ambient pressure to the peak reflected over pressure. It drops within 11.7 milli-seconds to stagnation pressure and then decreases to ambient again within

200 milli-seconds.

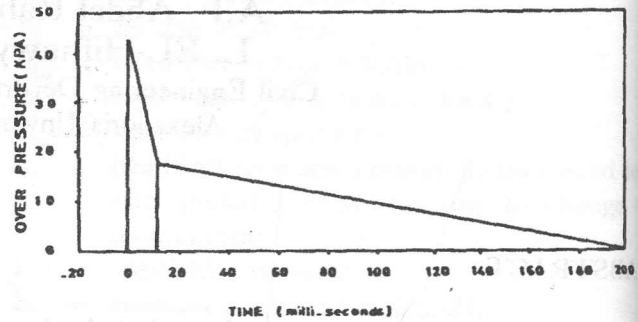


Figure 1-b. Averaged blast loading.

3. BUILDINGS ANALYZED

The structures analyzed (Figure 2) are shear buildings resting on shallow or deep foundation.

The pulse load described in Figure (1) applied to the structure on flexible foundation, yields the displacements. These are given by the relative displacements,  $u_1$ , and the base displacements  $u_b, \Psi$  for which the equilibrium conditions can be written as

$$[m] \{\ddot{u}\} + [c] \{\dot{u}\} + [k] \{u(t)\} = \{p(t)\} \quad (1)$$

in which  $\{u\} = \langle u_1 \ u_2 \ u_3 \ \dots \ u_N; \ u_b \ \Psi_b \rangle^T$  and matrices  $[m]$ ,  $[c]$  and  $[k]$  for the soil structure interaction system are:

$$[m] = \begin{bmatrix} [m] & \{m\} & \{mh\} \\ \{m\}^T & m_b + \sum_1^N m_i & \sum_1^N m_i h_i \\ \{mh\}^T & \sum_1^N m_i h_i & I_t + \sum_1^N m_i h_i^2 \end{bmatrix}$$

$$[c] = \begin{bmatrix} [c] & \{0\} & \{0\} \\ \{0\}^T & c_{uu} & c_{u\Psi} \\ \{0\}^T & c_{\Psi u} & c_{\Psi\Psi} \end{bmatrix}$$

$$[K] = \begin{bmatrix} [k] & \{0\} & \{0\} \\ \{0\}^T & k_{uu} & k_{u\Psi} \\ \{0\}^T & k_{\Psi u} & k_{\Psi\Psi} \end{bmatrix}$$

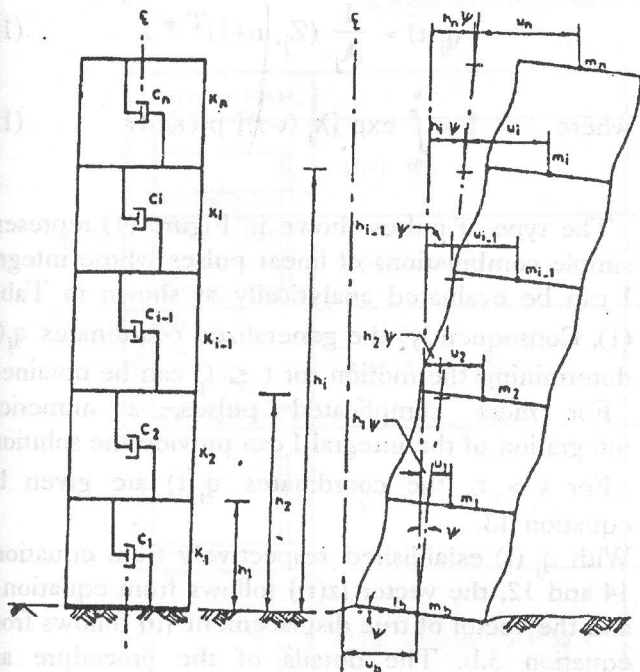


Figure 2. Model of building-foundation system.

The matrices [c] and [k] list all the stiffness and damping constants of the structure, [m] is the diagonal mass matrix of the structure, and {0} is the null vector. Also in Equation 1,  $I_t = \sum_{i=1}^N I_i + I_b$

The load vector {p(t)} contains the pulse load impacting the i-th floor of the analyzed building.

#### 4. SOLUTION OF IMPACT PROBLEMS USING THE COMPLEX EIGENVALUE APPROACH

The solution of equations (1) is facilitated by transforming them into 2n reduced differential equations of the first order (15)

$$A\dot{z} + Bz = F(t) \tag{2}$$

in which

$$A = \begin{bmatrix} 0 & m \\ m & c \end{bmatrix} \quad B = \begin{bmatrix} -m & 0 \\ 0 & k \end{bmatrix} \tag{3-a}$$

and

$$z = \begin{Bmatrix} \dot{u} \\ u \end{Bmatrix} \quad F(t) = \begin{Bmatrix} 0 \\ p(t) \end{Bmatrix} \tag{3-b}$$

The vector z comprises the vector of velocities  $\dot{u}$  and the vector of displacements u and hence its order is 2n.

For the solution of the response to pulse loading, free vibration has to be analyzed first.

For free vibration  $F(t) = 0$  and a particular solution to equation (2) can be written as:

$$z(t) = \exp(\lambda t) Z \tag{4}$$

in which  $\lambda$  is a complex eigenvalue to be determined and Z is a complex eigenvector independent of time. Denoting the identity matrix I and substituting equation (4) into equation (2), the eigenvalue problem is obtained in the following form:

$$(-A^{-1} B - \lambda I) Z = 0 \tag{5}$$

The solution of equation (5) by means of suitable subroutine yields 2n eigenvalues  $\lambda_j$  and corresponding eigenvectors  $Z_j$  for  $j=1,2,\dots, 2n$ . (The solution and a suitable subroutine are described in more detail in Ref. 11). The eigenvalues come out in complex conjugate pairs with corresponding pairs of complex conjugate modes. All eigenvectors can be assembled in a square modal matrix Z, having the individual eigenvectors as columns. The eigenvectors are orthogonal with the following orthogonality conditions for damped modes:

$$Z^T A Z = A_j \tag{6-a}$$

$$Z^T B Z = -B_j \tag{6-b}$$

in which  $A_j$  and  $B_j$  are diagonal matrices; the elements  $B_j = \lambda_j A_j$ .

The response to a given pulse can be obtained from equation (2) by means of the complex eigenvectors. Using the linear transformation:

$$z(t) = Z q(t) \tag{7}$$

in which the components of the vector q(t),  $q(t) = q_j$  are function of time with  $j=1,2,\dots,2n$ , equation (2) becomes:

$$A Z \dot{q} + B Z q = F(t) \tag{8}$$

Premultiplying by  $Z^T$  and applying the orthogonality conditions, equation (8) reduces to:

$$A_j \dot{q}_j - B_j q_j = Z^T F(t) \quad (9)$$

Since both  $A_j$  and  $B_j$  are diagonal matrices, equations (9) decouple into independent differential equations of the first order:

$$\dot{q}_j - \lambda_j q_j = f_j(t)/A_j \quad j = 1, 2, \dots, 2n \quad (10)$$

in which the functions of time  $f_j(t)$  are:

$$f_j(t) = Z_j^T F(t) \quad (11)$$

The complete solution to equation (10) is established as a sum of the homogeneous solution, given by the initial condition  $q_j(0)$ , and a particular integral of the nonhomogeneous equation. Thus, the complete solution for  $q_j$  is:

$$q_j(t) = q_j(0) \exp(\lambda_j t) + \frac{1}{A_j} \int_0^t \exp[\lambda_j(t-\tau)] f_j(\tau) d\tau \quad (12)$$

The first term of equation 12 defines the response due to initial conditions which are assumed to be zero; the second part of equation 12 describes the response during the application of the pulse ( $t \leq t_p$ ). The response for the time exceeding the duration of the pulse ( $t > t_p$ ) is given by

$$q_j(t) = q_j(t_p) \exp[\lambda_j(t-t_p)] \quad (13)$$

The integral in equation 12 has to be evaluated for a specific time history  $P(t)$  and hence  $f_j(t)$  given by equation 11. The length of the load vector  $\{F(t)\}$  is equal to  $2n$ , where  $n$  = number of degrees of freedom of the multi-storey shear building.

Consequently, if the impact load is applied at the  $i$ -th floor, the load vector of equation 3-b takes the form:

$$\{F(t)\}^T = \{ \underbrace{0 \ 0 \ \dots \ 0}_n, \underbrace{0 \ 0 \ p(t)}_{n+1}, \underbrace{0 \ \dots \ 0}_{2n} \}$$

Then the second term of equation 12 becomes

$$q_j(t) = \frac{1}{A_j} (Z_j, n+1)^T * I \quad (14)$$

where 
$$I = \int_0^t \exp[\lambda_j(t-\tau)] p(\tau) d\tau \quad (15)$$

The type of pulses shown in Figure (1) represent simple combinations of linear pulses whose integral  $I$  can be evaluated analytically as shown in Table (1). Consequently, the generalized coordinates  $q_j(t)$  determining the motion for  $t \leq t_p$  can be obtained.

For more complicated pulses, a numerical integration of the integral  $I$  can provide the solution.

For  $t > t_p$  the coordinates  $q_j(t)$  are given by equation 13.

With  $q_j(t)$  established respectively from equations 14 and 12, the vector  $\{z(t)\}$  follows from equation 7 and the vector of true displacement  $\{u\}$  follows from equation 3.b. The details of the procedure are presented in the following subchapters.

#### 4.1 Case of vehicle impact

(1) For  $0 < t \leq t_1$   $\bar{t} = t$

Assuming the initially at rest condition the first part of equation 12 vanishes, and the generalized coordinates  $q(t)$  are determined from the second part as follows (Figure (1-a, 3-a))

$$q_j(t) = \frac{[Z]^T}{[A_j]} \times \frac{P_o}{(-\lambda_j \cdot t_1)} \left[ \bar{t} + \frac{1.0}{\lambda_j} - \frac{e^{\lambda_j \bar{t}}}{\lambda_j} \right] \quad (16-a)$$

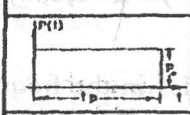
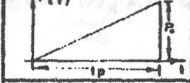
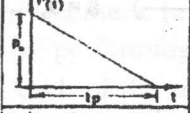
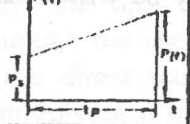

(ii) For  $t_1 < t \leq t_2$   $\bar{t} = t - t_1$

In this step, the solution is a sum of the homogeneous solution (first part of equation 13) and the particular solution (second part of equation 13) as follows:

$$q_j(t) = q_j(t_1) \exp(\lambda_j \bar{t}) + \frac{P_o}{(t_2 - t_1)} \frac{[Z]^T}{[A_j]} \frac{1}{\lambda_j} \left[ e^{\lambda_j \bar{t}} - 1 \right] (t_2 - t_1) + \bar{t} + \frac{1.0}{\lambda_j} - \frac{e^{\lambda_j \bar{t}}}{\lambda_j} \quad (16.b)$$



Table 1. Function I for main types of pulses.

TYPE OF PULSF	P(t)	CONVOLUTION BY DIRECT INTEGRATION
	$P(t) = P_0$	$I = P_0 \left\{ \frac{\exp(\lambda t) - 1.0}{\lambda} \right\}$
	$P(t) = P_0 \cdot \frac{t}{t_p}$	$I = \frac{P_0}{(\lambda + 1/t_p)} \cdot \left( t + \frac{1.0}{\lambda} - \frac{\lambda t}{\lambda} \right)$
	$P(t) = P_0 \cdot \frac{(t_p - t)}{t_p}$	$I = \frac{P_0}{(\lambda + 1/t_p)} \left\{ t_p (e^{\lambda t} - 1.0) + t + \frac{1.0}{\lambda} - \frac{\lambda t}{\lambda} \right\}$
	$P(t) = P_2 + (P_1 - P_2) \cdot \frac{t}{t_1}$	$I = \left\{ \frac{P_2}{\lambda} (e^{\lambda t} - 1.0) + \left( t + \frac{1.0}{\lambda} - \frac{\lambda t}{\lambda} \right) \cdot \left( \frac{P_2 - P_1}{\lambda t_1} \right) \right\}$
	$P(t) = P_1 + (P_2 - P_1) \cdot \frac{t - t_1}{t_1}$	$I = \left\{ \frac{P_2}{\lambda} (e^{\lambda t} - 1.0) + \left( \frac{P_2 - P_1}{\lambda t_1} \right) \left( t + \frac{1.0}{\lambda} - \frac{\lambda t}{\lambda} \right) \right\}$

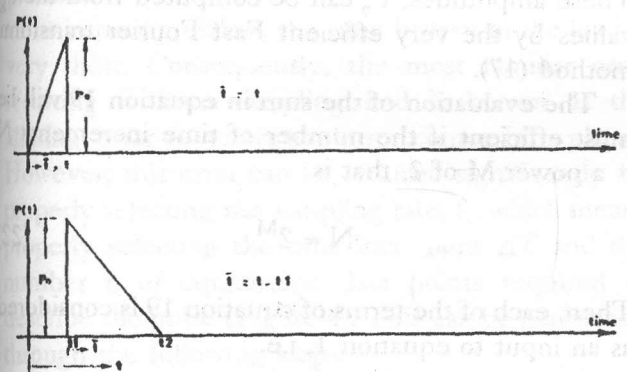


Figure 3-a. Analyzed vehicle load.

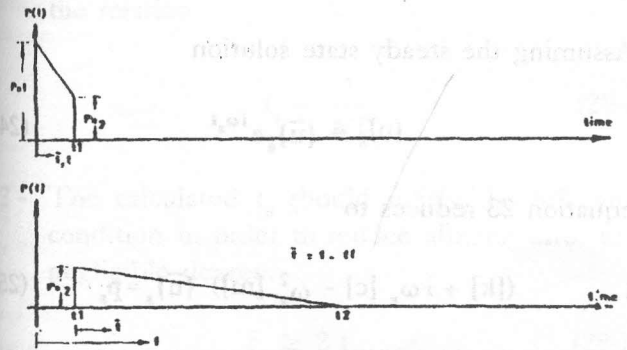


Figure 3-b. Analyzed blast load.

(iii) For  $t > t_2$   $\bar{t} = t - t_2$

The generalized coordinates are given by the first part of equation 13 describing the response for time exceeding the duration of the pulse (state of free vibration with initial conditions)

$$q_j(t) = q_j(t_2) \exp(\lambda_j \bar{t}) \tag{16.c}$$

4.2. Case of blast load

(i) For  $0 < t \leq t_1$   $\bar{t} = t$

The initially "at rest" condition is assumed; and the generalized coordinates are obtained from the second part of equation 13 as follows (Figure 3-b):

$$q_j(t) = \frac{[Z]^T}{[A_j]} \left[ \frac{P_{o1}}{\lambda_j} (e^{\lambda_j \bar{t}} - 1) + \frac{(P_{o1} - P_{o2})}{(\lambda_j t_1)} \left[ \bar{t} + \frac{1}{\lambda_j} - \frac{e^{\lambda_j \bar{t}}}{\lambda_j} \right] \right] \tag{17-a}$$

(ii) For  $t_1 < t \leq t_2$   $\bar{t} = t - t_1$

In this step of the analysis, the generalized coordinates are the sum of both parts of equation 13 giving

$$q_j(t) = q_j(t_1) \exp(\lambda_j \bar{t}) + \frac{[Z]^T P_{o2}}{[A_j] (t_2 - T_1) \lambda_j} \left[ (t_2 - t_1)(e^{\lambda_j \bar{t}} - 1) + \bar{t} + \frac{1}{\lambda_j} - \frac{e^{\lambda_j \bar{t}}}{\lambda_j} \right] \quad (17-b)$$

(iii) For  $t > t_2$   $\bar{t} = t - t_2$

For time exceeding the duration of the pulse, the coordinates  $q_j(t)$  are described by the first term in equation 13 (i.e. state of free vibration with initial conditions) as follows

$$q_j(t) = q_j(t_2) \exp(\lambda_j \bar{t}) \quad (17-c)$$

With  $q_j(t)$  established respectively from equations 16 or 17, the vector  $\{z(t)\}$  containing the true displacements  $\{u\}$  follows from equations 7 and 3b. The  $i$ -th displacements component  $u_i$  of the vector  $\{u\}$  is equal to the  $(n+i)$ -the element of the vector  $\{z(t)\}$ , i.e.

$$u_i(t) = z_{n+i}(t) \quad (18)$$

### 5. SOLUTION OF IMPACT PROBLEMS USING THE COMPLEX RESPONSE ANALYSIS (FOURIER METHOD)

The equations of motion of the soil-structure interaction system, equation 1, can be solved in the frequency domain using Fourier transform method (complex response method). For this purpose, each input force  $P(t)$  is assumed to be given for an even number,  $N$ , of equidistant points in the time domain as

$$P_K = P(k, \Delta t), \quad k = 0, 1, 2, \dots, N-1 \quad (19-a)$$

and is expanded into a continuous function by the

trigonometric interpolation formula

$$P_K(t) = \sum_{s=0}^{N-1} P_s \exp(i \frac{2\pi ks}{N}) \quad k=0, 1, \dots, (N-1) \quad (19-b)$$

$P_s$  are complex amplitudes in the frequency domain called Fourier transforms of  $P_k(t)$  and are defined as

$$P_s = \frac{1}{N} \sum_{k=0}^{N-1} P_k \exp(-i \frac{2\pi sk}{N}) \quad s=0, 1, \dots, (N-1) \quad (20)$$

the power  $i \frac{2\pi ks}{N}$  may be written as  $i \omega_s t$  where  $\omega_s$  are the frequencies

$$\omega_s = \frac{2\pi s}{N \Delta T} = \Delta \bar{\omega} \cdot s \quad (21)$$

where  $\Delta \bar{\omega}$  and  $\Delta \bar{\omega} (N-1)$  are the lowest and highest frequencies to be considered in the analysis. These amplitudes,  $P_s$  can be computed from the  $P_k$  values by the very efficient Fast Fourier transform method (17).

The evaluation of the sum in equation 19 will be most efficient if the number of time increments  $N$  is a power  $M$  of 2, that is

$$N = 2^M \quad (22)$$

Then, each of the terms of equation 19 is considered as an input to equation 1, i.e.

$$[m] \{\ddot{u}\}_s + [c] \{\dot{u}\}_s + [k] \{u\}_s = \{p_s\} e^{i\omega_s t} \quad (23)$$

Assuming the steady state solution

$$\{u\}_s = \{\bar{u}\}_s e^{i\omega_s t} \quad (24)$$

equation 23 reduces to

$$([k] + i \omega_s [c] - \omega_s^2 [m]) \{\bar{u}\}_s = \{p_s\} \quad (25)$$

Equation 25 constitutes a set of linear equations which can be solved for the complex displacement

amplitudes  $\{\bar{u}\}_s$ . Then,  $\{u\}_s$  follows from equation 24. The complete response in the time domain follows by superposition, of the response components  $\bar{u}_s$ , i.e.,

$$\{u\} = \sum_{s=0}^{N-1} \{u\}_s = \sum_{s=0}^{N-1} \{\bar{u}\}_s e^{i\omega_s t} \quad (26)$$

Thus, the displacement  $\{u\}$  in the time domain can be obtained by performing an inverse Fast Fourier transform on each of the terms of  $\{\bar{u}\}_s$ .

In summary, the time history response can be computed through the use of Fourier transforms by (1) finding the direct transform of the excitation forces, (2) multiplying it by the transfer function

$$H(\omega) = ([k] + i\omega_s [c] - \omega_s^2 [m])^{-1} \quad (27)$$

and (3) obtaining the inverse transformation of the product.

For impact problem, the time history of the load is very short. Consequently, the most familiar error resulting is from sampling and is known as the aliasing error (overlapping error comes into place). However, this error can be reduced significantly by properly selecting the sampling rate,  $f_s$ , which means properly selecting the time increment  $\Delta T$  and the number  $n$  of equidistant data points required to describe the pulse (Figure 4). This can be performed through the following steps:

1 - Choose the time increments  $\Delta T$ , and determine the corresponding sampling frequency,  $f_s$ , from the relation.

$$f_s = \frac{1}{\Delta T} \quad (28-a)$$

2 - The calculated  $f_s$  should satisfy the following condition in order to reduce aliasing error to a negligible degree.

$$f_s \geq 2 f_{max} \quad (28-b)$$

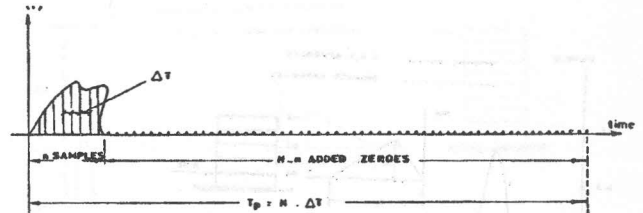


Figure 4-a. One Period of the load.

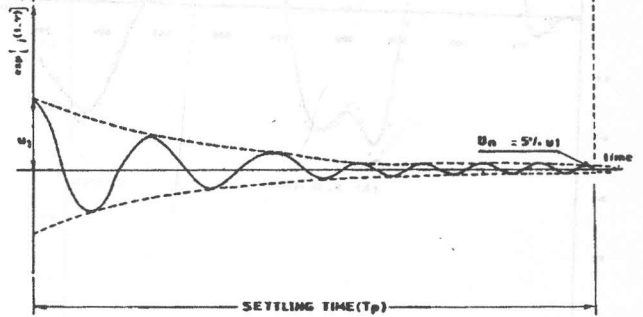


Figure 4.b. Unit impulse response function.

Where  $f_{max}$  is the largest frequency component of the Fourier transform of the time function  $p(t)$ . If not, choose  $\Delta T$  smaller, i.e., sample faster.

3 - Determine the required number  $n$  of equidistant data points describing the pulse from the relation

$$t_p = n \cdot \Delta T \quad (28-c)$$

where  $t_p$  = duration of the pulse load.

When using the discrete Fourier transform, it is important to remember that it is based on the assumption that the load  $p(t)$  is periodic. To minimize errors in the analysis of non-periodic loads such as impact loads, or pulses, the pulse load of duration  $t_p = n \cdot \Delta T$  is assumed to be periodic with a period  $T_p = N \cdot \Delta T$ , where  $N$  is the total number of equidistant samples describing one period of the load. This is performed by adding  $(N-n)$  extra zeroes to the sampled data representing the pulse load (Figure (4-a)) as follows.

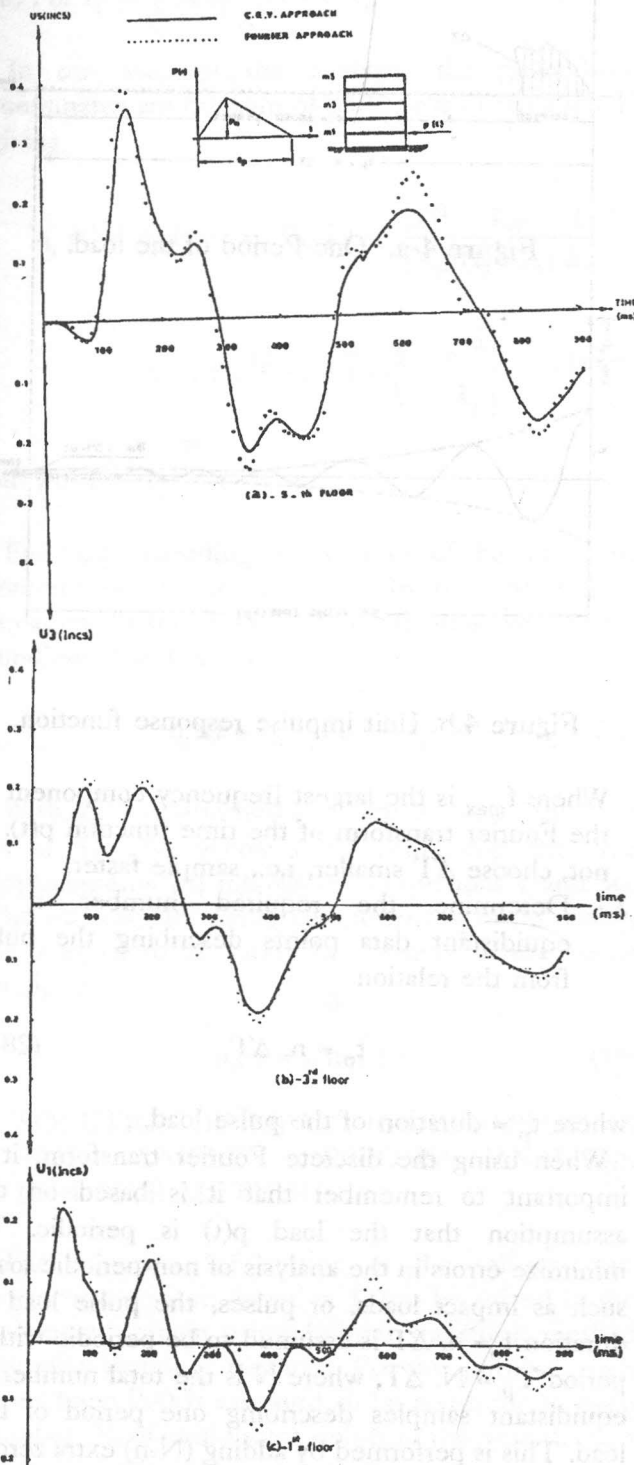


Figure 5. Damped response of a 5 storey shear building due to vehicle impact  $U_5, U_3, U_1$ , storey deformations of fifth, third, and first floor respectively, (displ. inches, time in milliseconds,  $T_p/T_{pt}=0.265$ ) \*1 in = 0.0254 m).

$$P_K = P \quad 0 \leq k \leq n-1 \quad (29-a)$$

$$P_K = 0 \quad n \leq k \leq N-1 \quad (29-b)$$

*Determination of the number of zeroes*

As indicated by equation 25, the steady state component of the response in the frequency domain is given by

$$\{\bar{u}\} = \{[k] + i\omega_s[c] - \omega_s^2[m]\}^{-1} \{P_s\} \quad (30-a)$$

or

$$\{\bar{u}\}_g = H(\omega) \{P_s\} \quad (30-b)$$

Equation 30.b represents a simple multiplication in the frequency domain which is equivalent to a convolution in the time domain (16) i.e.

$$\int_0^t h(t-\tau)P(\tau)d\tau < > (H(\omega)) * \{P_s(\omega)\} \quad (31)$$

where  $h(t-\tau)$  is the unit impulse response function of a system defined as the response of the system to an impulse of unit magnitude applied at time  $t=\tau$ . The unit impulse response function can be expressed in terms of complex eigenvectors for a damped system as follows

$$h(t-\tau) = \frac{1}{A_j} \exp [\lambda_j (t-\tau)] \quad (32)$$

To avoid convolution errors in performing the multiplication in equation 30-b, the two convoluted sequences must have the same length in the time domain, i.e. the unit impulse response of the system,  $h(t-\tau)$ , and the pulse load,  $p(t)$  must have the same length  $T_p$  in the time domain (Figure 4). This implies adding  $(N-n)$  extra zeroes to the load sequence. The number of these added extra zeroes can be obtained by determining the length of the unit impulse response,  $h(t-\tau)$ , in the time domain so that the amplitude of  $h(t-\tau)$ , is reduced to 5% of its initial value from equation (32). That is to say zeroes are added to the pulse load sequence until the settling time  $T_p$  of the structure is reached.



6. EXAMPLES

Five-, ten- and fifteen storey shear buildings are examined. Properties of the buildings are given in Table (2). Five-storey and ten-storey shear buildings, are supported by shallow foundations, while fifteen-storey shear building is supported by a deep pile foundation.

The vehicle impact load is assumed to impact horizontally, the first floor of the analysed building. The blast impact load is assumed to impact the top floor of the considered buildings in the horizontal direction. For each case, the response at the top, intermediate, and first floors are determined (Figures 5 to 10).

For the case of vehicle impact load applied at first floor of the buildings, it can be seen from Figures (5 to 7) that the storey deformations are not in phase together. This indicates that the load in this case seems to excite modes higher than the first mode of vibration (Figure 11). For the five and ten storey buildings, the second mode of vibration seems to control the response (one inflection point), while for the fifteen storey building the third mode may be controlling the response (two inflection points).

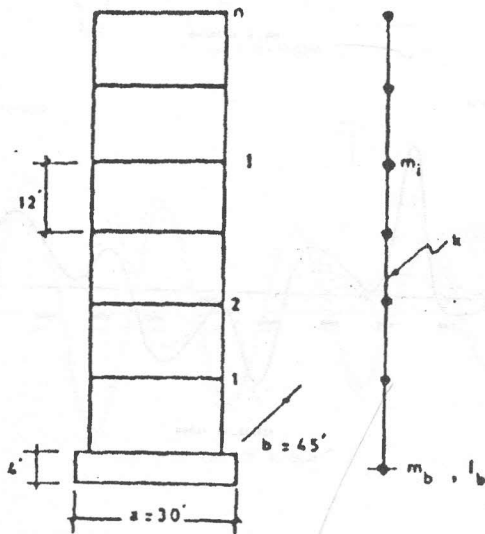


Table (2)

Building Properties (n floors)			
$m_1$	4472.05 SLUGS	=	65376.00 kg
$m_b$	25155.28 SLUGS	=	367740.00 kg
$I_b$	1920180.40 SLUGS. ft <sup>2</sup>	=	2607856.30 kgm <sup>2</sup>
$k$	17.36 x 10 <sup>6</sup> lb/ft	=	253.66 N/m
$R_n = \sqrt{a b / \pi}$	20.73ft	=	6.32 m

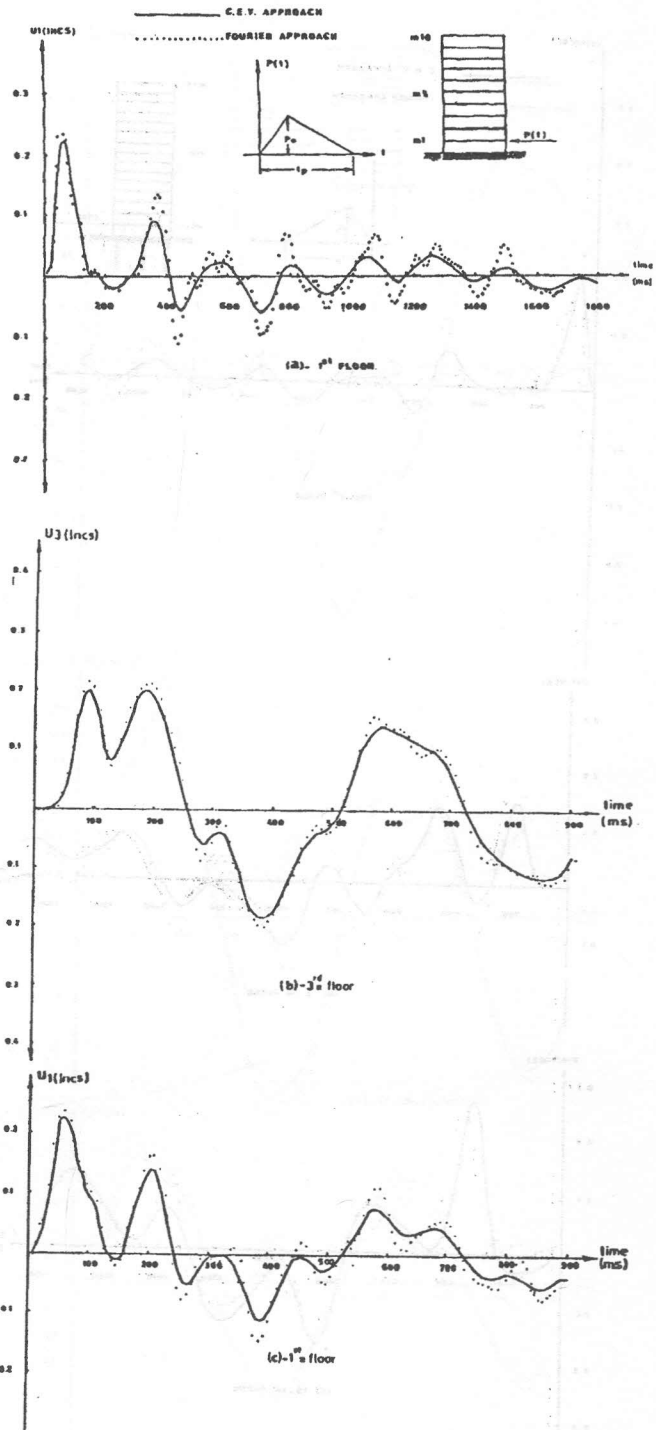


Figure 6. Damped response of a 10 storey shear building due to vehicle impact  $U_1$ ,  $U_5$ ,  $U_{10}$  storey deformations of first, fifth, and tenth floor respectively, (displ. in inches, time in milliseconds,  $t_p/\Gamma_{pt}=0.125$ ), (1 in=0.0254 m).

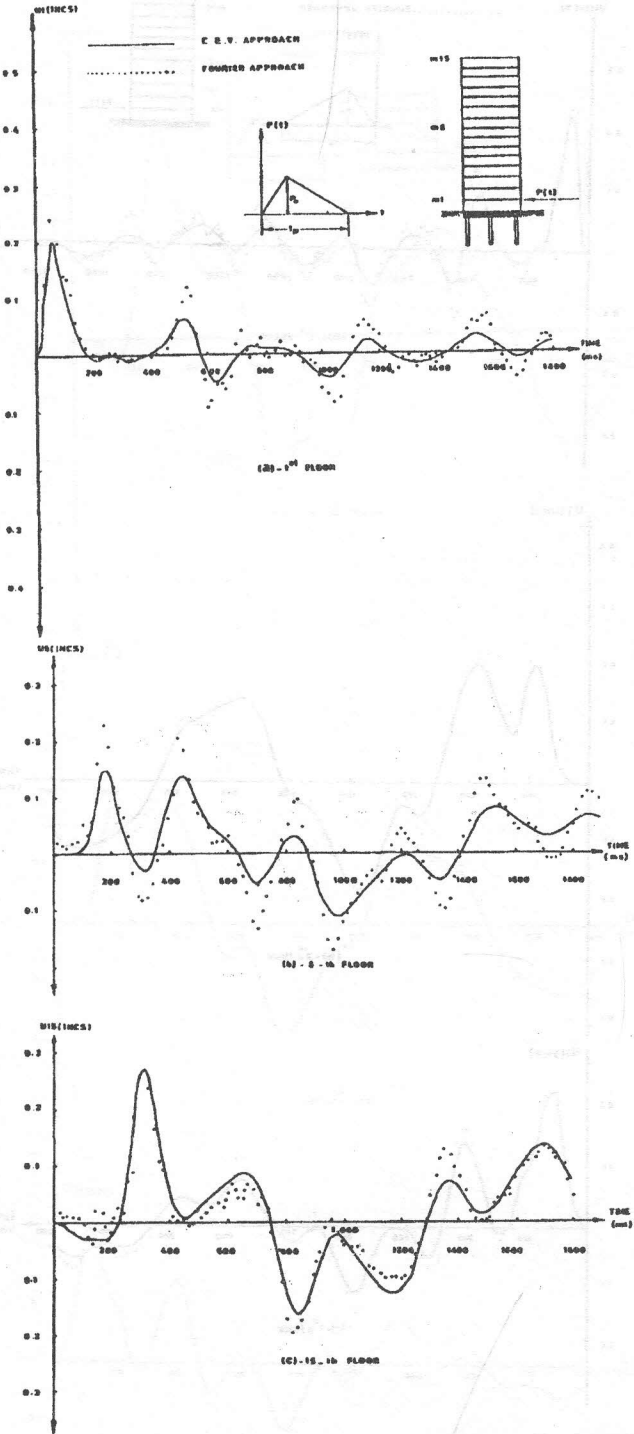


Figure 7. Damped response of a 15 storey shear building due to vehicle impact  $U_1, U_8, U_{15}$ , storey deformations of first, eighth, and fifteenth floor respectively, (displ. in inches, time in milliseconds,  $t_p/T_{pt}=0.093$ ), (1 in=0.0254 m).

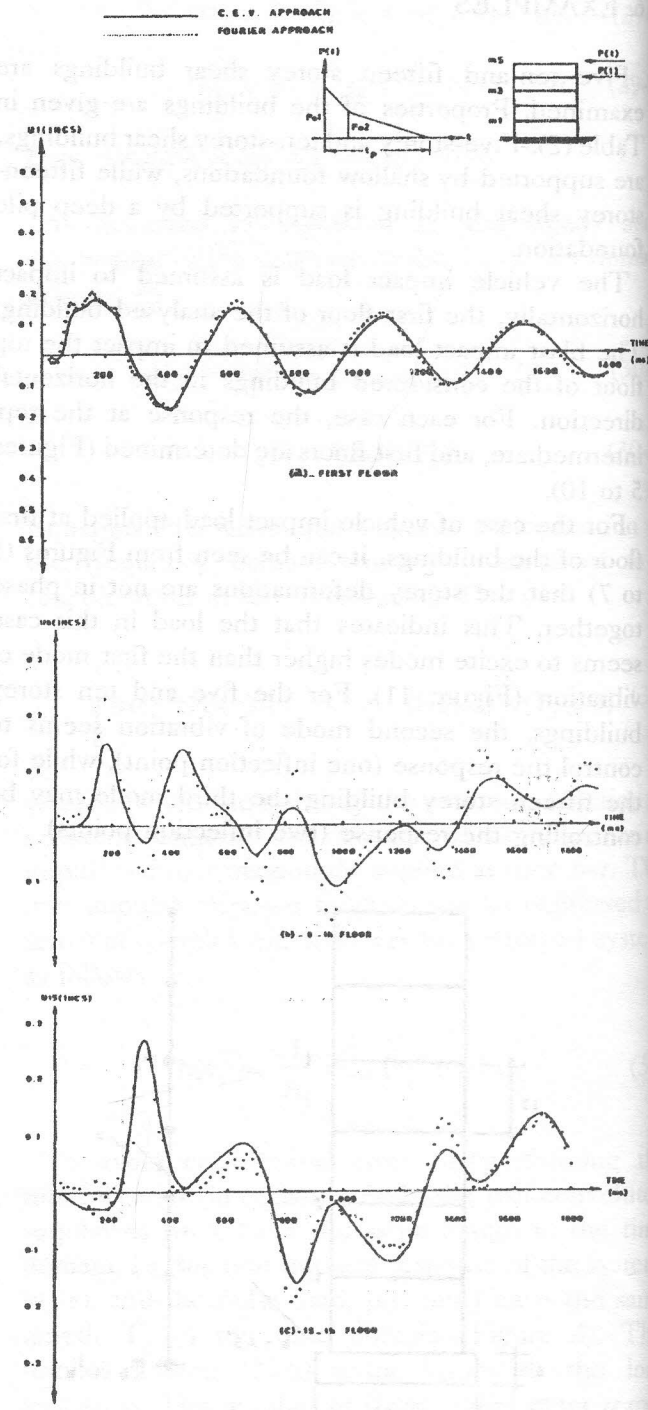


Figure 8. Damped response of a 5 storey shear building due to vehicle impact  $U_1, U_3, U_5$ , storey deformations of first, third, and fifth floor respectively, (displ. in inches, time in milliseconds,  $t_p/T_{pt}=0.441$ ), (1 in=0.0254 m).

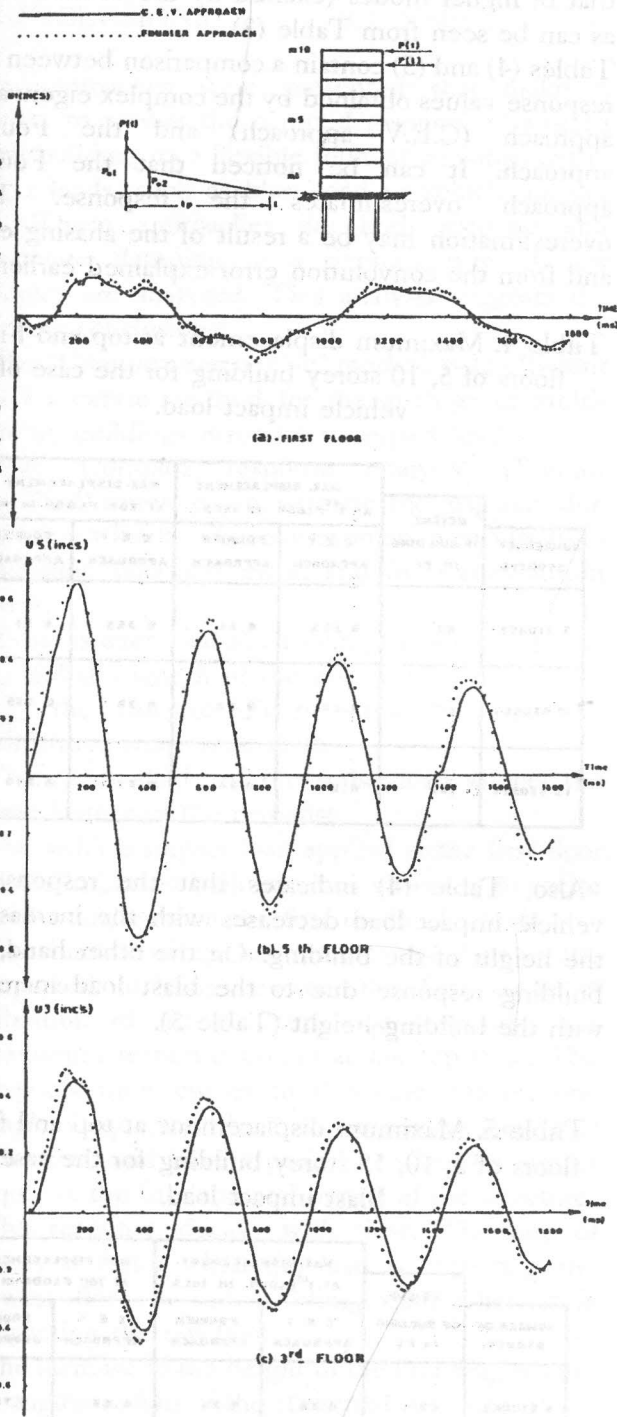


Figure 9. Damped response of a 10 storey shear building due to vehicle impact  $U_{10}$ ,  $U_5$ ,  $U_1$ , storey deformations of tenth, fifth, and first floor respectively, (displ. in inches, time in milliseconds,  $t_p/T_{pt}=0.209$ ), (1 in=0.0254 m).

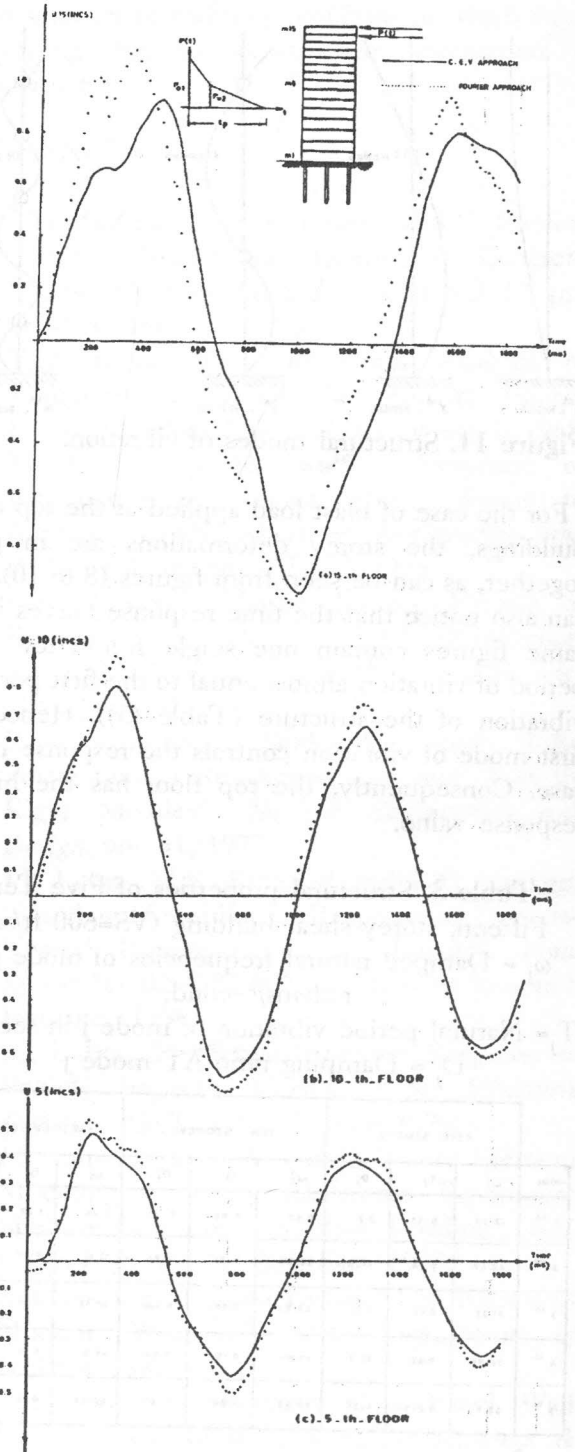


Figure 10. Damped response of a 15 storey shear building due to vehicle impact  $U_{15}$ ,  $U_8$ ,  $U_1$ , storey deformations of first, fifth, and tenth floor respectively, (displ. in inches, time in milliseconds,  $t_p/T_{pt}=0.125$ ), (1 in=0.0254 m).

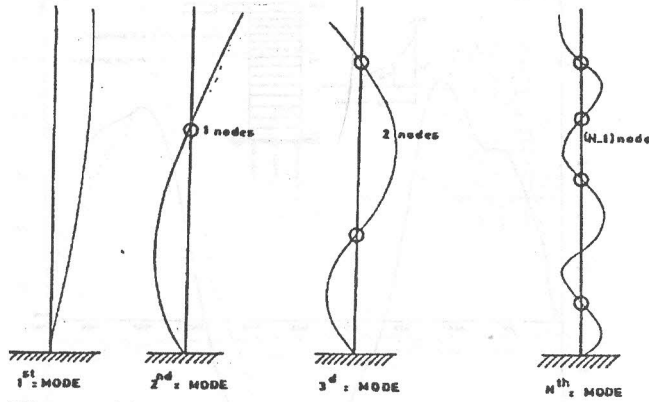


Figure 11. Structural modes of vibration.

For the case of blast load applied at the top of the buildings, the storey deformations are in phase together, as can be seen from figures (8 to 10). One can also notice that the time response curves in the same figures contain one single frequency and a period of vibration almost equal to the first period of vibration of the structure (Table (3)). Hence, the first mode of vibration controls the response in this case. Consequently, the top floor has the highest response value.

Table 3. Structural properties of Five Ten, Fifteen, storey shear building (VS=600 ft/sec)

$\omega_j$  = Damped natural frequencies of mode j in radians/second,

$T_j$  = Natural period vibration of mode j in seconds,

$D_j$  = Damping ratio AT mode j

MODE	FIVE STOREY			TEN STOREY			FIFTEEN STOREY		
	$\omega_j$	$T_j$	$D_j$ %	$\omega_j$	$T_j$	$D_j$ %	$\omega_j$	$T_j$	$D_j$ %
1 <sup>st</sup>	13.07	0.45	3.8	6.57	0.95	2.83	4.06	1.29	0.645
2 <sup>nd</sup>	40.45	0.15	53.8	26.90	0.23	4.28	18.18	0.24	3.93
3 <sup>rd</sup>	51.32	0.12	5.56	44.62	0.14	6.06	30.12	0.21	5.19
4 <sup>th</sup>	76.29	0.08	26.7	61.96	0.10	7.93	41.20	0.15	8.06
5 <sup>th</sup>	82.1	0.076	6.96	77.00	0.08	9.33	49.25	0.12	11.0

Also, Figures (5 to 10) show that the structural response in both cases of loading decays with time. This decay is slower in the case of the blast load impacting the top floor of the buildings. This may be due to the fact that the first mode of vibration (excited by the blast load) has less damping than

that of higher modes (excited by the vehicle load), as can be seen from Table (3).

Tables (4) and (5) contain a comparison between the response values obtained by the complex eigenvalue approach (C.E.V approach) and the Fourier approach. It can be noticed that the Fourier approach overestimates the response. This overestimation may be a result of the aliasing error and from the convolution error explained earlier.

Table 4. Maximum displacement at top and First floors of 5, 10 storey building for the case of vehicle impact load.

NUMBER OF STOREYS	HEIGHT OF BUILDING IN FT.	MAX. DISPLACEMENT AT 1 <sup>st</sup> FLOOR IN INCS		MAX. DISPLACEMENT AT TOP FLOOR IN INCS	
		C. E. V. APPROACH	FOURIER APPROACH	C. E. V. APPROACH	FOURIER APPROACH
5 STOREY	62'	0.225	0.24	0.355	0.39
10 STOREY	122'	0.22	0.23	0.30	0.365
15 STOREY	182'	0.2	0.24	0.275	0.270

Also, Table (4) indicates that the response to vehicle impact load decreases with the increase in the height of the building. On the other hand, the building response due to the blast load increases with the building height (Table 5).

Table 5. Maximum displacement at top and first floors of 5, 10, 15 storey building for the case of Blast impact load.

NUMBER OF STOREY	HEIGHT OF BUILDING IN FT	MAX. DISPLACEMENT AT 1 <sup>st</sup> FLOOR IN INCS		MAX. DISPLACEMENT AT TOP FLOOR IN INCS	
		C. E. V. APPROACH	FOURIER APPROACH	C. E. V. APPROACH	FOURIER APPROACH
5 STOREY	62	0.19	0.28	0.66	0.74
10 STOREY	122	0.13	0.16	0.81	0.93
15 STOREY	182	0.16	0.24	0.93	1.15



## 7. CONCLUSIONS

Two approaches were presented that make it possible to predict the damped response of a multi storey building on a flexible foundation subjected to impact loads, such as blast load or vehicle impact load. These approaches are both accurate and incorporate damping in a rigorous way. A few examples are analyzed. This analysis suggests the following conclusions:

- The "Complex eigenvalue" method is an efficient and accurate method for the analysis of multi-storey buildings response to impact loads.
- The "Complex response analysis" (Fourier method) tends to overestimate the response due to impact loads. This overestimation results from sampling (aliasing) error, and from convolution error.
- If care is exercised in choosing the sampling rate,  $f_s$ , and the length of the assumed periodic load,  $T_p$ , the discrete Fourier transform can be performed more accurately.
- The exact shape of the pulse load affects the time history of the response.
- The vehicle impact load applied at the first floor of the impacted buildings was observed to excite modes higher than the first mode of vibration.
- The blast load applied at the top floor of the impacted buildings excites the first mode of vibration of the structure. Consequently, the maximum response occurs at the top floor. The response-time curves in this case contain one single frequency (the first natural frequency of vibration) and have a period of vibration almost equal to the fundamental period of the structure.
- The response decays with time. The rate of decay is faster when the load is impacting the lowest floor of the building, than when it is impacting the top floor.
- The increase of the height of the building, results in augmentation of the structural response of the impacted building when the load is applied at its top. On the other hand, for the case of impact load applied at the bottom floor of the building, the higher is the building, the smaller is its peak response.
- Both the complex eigenvalue approach and the Fourier approach are very suitable methods for

the solution of collision problems in which large damping due to soil-structure interaction is anticipated.

## REFERENCES

- [1] TH. Zimmermann, B. Reborá and C. Rodrez, "Aircraft Impact on Reinforced Concrete Shells", *Computers and Structures*, vol. 13, pp. 263-274, 1981.
- [2] Y.D. Riera, "On the Stress Analysis of Structures Subjected To Aircraft Impact Forces", *Nuclear Eng. and Design*, vol. 8, 1968.
- [3] M. Scalk and H. Wolfel, "Response of Equipment in Nuclear Power Plants to Airplane Crash," *Nuclear Engineering and design*, vol. 38, pp. 567-582, 1976.
- [4] F.V. Vassallo, "Missile Impact Testing of Reinforced Concrete Panels", *CLASPAN Report No. HC- 5609-D-1 CALSPAN Corp.*, Buffalo, N.Y., Jan, 1975.
- [5] R. Guerand and A. Soklowsky, "Study of the Perforation of Reinforced Concrete Slabs by Rigid Missiles", *Nuclear Engineering and Design*, vol. 41, 1977.
- [6] J.J. Labra, M.E. Bronslad and L.C. Calcote, "Simulated Steel Barrier Response to Tornado-Tossed Passenger Vehicle Impact", *Final Report No. 02-4583-002*, South West Research Institute, Texas, 1977.
- [7] J.J. Labra, "Protective Structure Response to Vehicle Impact", *Journal of the Structural Division, ASCE*, vol. 105, June 1979.
- [8] M. Callieros, and J.P. Walsh, "Finite Element Modeling of Army Electronic Equipment Shelters Subjected to blast Loading", *BRL Contract Report No. 281*, Dec, 1975.
- [9] S. Glasstone, P.J. and Dolan, "The Effects of Nuclear Weapons", *U.S. Department of Defense*, 1977.
- [10] M.H. Klaus, "Response of a Panel Wall Subjected to Blast Loading", *Computers & Structures*, vol. 21, pp 129-133, 1985.
- [11] L. El Hifnawy, and M. Novak, "Effect of Soil-Structure Interaction on Damping of Structures", *Department Report No. BLWT-4-1982*, University of Western Ontario, October 1982.

[12] L. El Hifnawy, and M. Novak, "Vibration of Hammer Foundations", *Soil Dynamics and Earthquake Engineering*, vol. 2, No. 1, 1983.

[13] L. El Hifnawy, and M. Novak, "Response of hammer Foundations to Pulse Loading", *Int. J. Soil Dynamics and Earthquake Engineering*, vol. 3, No. 3, 1984.

[14] L. El Hifnawy, and M. Novak, "Effect of Foundation Flexibility on Dynamic Behaviour of Buildings", *Eight World Conference on Earthquake Engineering, San Francisco, July, 1984*.

[15] R.A. Frazar, W.J. Duncan and A.R. Collar, "Elementary Matrices", *Cambridge University Press, London, England*, pp. 327, 1946.

[16] E.O. Brigham, *The Fast Fourier Transform*, Prentice-Hall, Inc., New Jersey, pp. 91-94, 1974.

[17] J.W. Cooley, and J.W. Tukey, "An Algorithm for Machine Calculation of Complex Fourier Series", *Math. Computation*, vol. 19, pp. 297-301, April 1965.

[18] W.M. Gentleman, and G. Sande, "Fast Fourier Transforms for Fun and profit", *AFIPS Proc. Fall Joint Comp. Conf.*, vol. 29, pp. 563-678, 1966.